

MERIDIONAL CIRCULATION AND SHEAR TURBULENCE IN LOW-MASS RGB STARS

A. Palacios¹, C. Charbonnel^{2,3}, S. Talon⁴ and L. Siess¹

Abstract. Red giant (RGB) stars in the field and in globular clusters present abundance anomalies that can not be explained by standard stellar evolution models. Some of these peculiarities, in particular those concerning lithium, carbon and nitrogen for stars more luminous than the bump, attest the presence of extra-mixing processes at play inside the stars. Although their nature remains unclear, rotation has often been invoked as a possible source for mixing inside RGB stars (Sweigart & Mengel (1979), Charbonnel (1995), Denissenkov & Tout (2000)). Much work has been done during the last decade on the description of rotation-induced mixing and on the transport of angular momentum and chemicals by meridional circulation and shear turbulence (Zahn 1992, etc ...). Within this framework, we present the first fully consistent computations of rotating low mass and low metallicity stars from the Zero Age Main Sequence (ZAMS) to the upper RGB. When self-consistent evolution of the internal distribution of angular momentum is taken into account, it is found that meridional circulation and shear instability by themselves are not able to produce the required amount of mixing to account for the observed abundance patterns.

1 Models and physical ingredients

We compute 3 models with initial mass $M_{\text{ini}} = 0.85 M_{\odot}$, and $Z = 10^{-3}$ (i.e. a typical globular cluster star). Model **A** is a non-rotating (standard) model, with no mixing outside of the convective regions. Model **B** is a slow rotator with an initial velocity $v_{\text{ZAMS}} = 5 \text{ km.s}^{-1}$, with solid body rotation in the convective envelope at all phases ($\Omega_{\text{CE}}(r) = \text{cst}$). Model **C** is a rapid rotator on the ZAMS ($v_{\text{ZAMS}} = 110 \text{ km.s}^{-1}$), undergoing main sequence magnetic braking (as in Pop I

¹ Institut d'Astronomie et d'Astrophysique - Université Libre de Bruxelles, Brussels (Belgium)

² Geneva Observatory, Sauverny (Switzerland)

³ CNRS (France)

⁴ Département de Physique - Université de Montréal, Montréal (Canada)

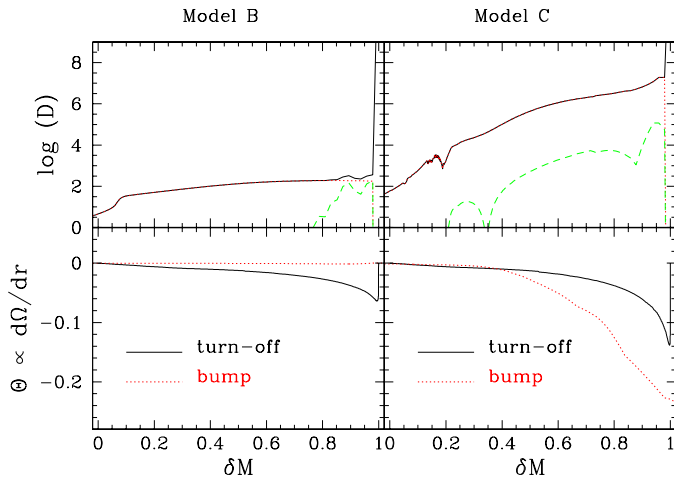


Fig. 1. *Upper panels* : Diffusion coefficient profiles (D_v - dotted; D_{eff} - dashed; $D_v + D_{\text{eff}}$ - solid) in rotating models **B** (left) and **C** (right) at the bump luminosity as a function of the scaled mass coordinate $\delta M = \frac{M_r - M_{\text{HBS}}}{M_{\text{BCE}} - M_{\text{HBS}}}$ ($\delta M = 1$ at the convective envelope base and 0 where $X = 10^{-7}$). *Lower panels* : Degree of differential rotation at the turn-off (solid lines) and at the bump (dotted lines).

stars) so as to obtain $v_{\text{turn-off}} = 3 \text{ km.s}^{-1}$. For this model we assume a uniform specific angular momentum distribution in the convective envelope beyond the turn-off ($\Omega_{\text{CE}}(r) \propto r^2$).

In our rotating models we consider the transport of angular momentum and chemicals by meridional circulation and shear turbulence, and use the formalism by Maeder & Zahn (1998). The prescriptions adopted for the vertical and horizontal turbulent diffusion coefficients, D_v and D_h are from Talon & Zahn (1997) and Mathis et al. (2004) respectively. The effective diffusion coefficient D_{eff} entering the transport equation for the chemicals is from Zahn (1992).

2 Diffusion coefficients and transport efficiency

Fig. 1 presents the profiles of the different diffusion coefficients in the rotating models **B** and **C** at the bump luminosity¹. The turbulence induced by the shear instability dominates the transport of chemicals in both models across the radiative zone. The mixing of chemicals is efficiently prevented at the bottom of the Hydrogen Burning Shell (HBS) ($D_{\text{tot}} \leq 10$ for $\delta M \leq 0$) by the presence of a

¹The bump luminosity corresponds to the point on the RGB when the outgoing HBS encounters the mean molecular weight discontinuity left by the deepening of the convective envelope during the 1st DUP. It is actually associated with a bump in the luminosity function.

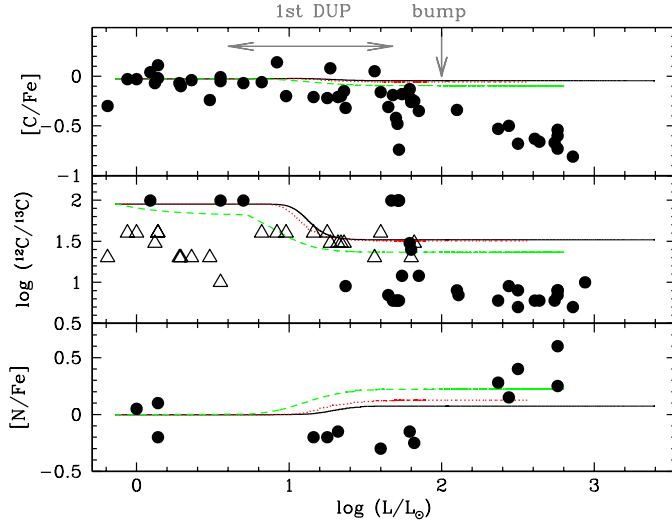


Fig. 2. Evolution of C, $^{12}\text{C}/^{13}\text{C}$ and N surface abundances as a function of the luminosity for models **A** (solid line), **B** (dotted line) and **C** (dashed line). Black dots and open triangles are measures and lower limits respectively for field stars with $-2 \leq [\text{Fe}/\text{H}] \leq -1$ by Gratton *et al.* (2000). Here we use the classical spectroscopic notation $[\text{X}/\text{Fe}] = \log(\text{X}/\text{Fe})_* - \log(\text{X}/\text{Fe})_{\odot}$.

large mean molecular weight gradient associated with the hydrogen combustion. The growth of shear turbulence in the region between the top of the HBS and the base of the convective envelope is favoured in the case of uniform specific angular momentum in the convective envelope, as already predicted by Sweigart & Mengel (1979) and Sills & Pinsonneault (2000). In this case, most of the angular momentum of the convective envelope is stored in its inner part during the dredge-up (DUP). When the convective envelope retreats after the completion of the 1st DUP, a large differential rotation (lower panels), and thus shear turbulence develops in the underlying newly radiative zone.

Let us mention that the difference in the adopted rotation law in the envelope is the main discriminating factor for the RGB evolution of angular momentum of models **B** and **C**. Having different initial velocities leads to different evolutions of the angular momentum on the main sequence but once the 1st DUP is completed, the outcoming angular momentum evolution (and mixing) does not depend anymore on these initial conditions (see Palacios *et al.* (2005) for further details).

3 Comparison with observations

In Fig. 2 we compare the evolution of the surface abundances of C and N, and that of $^{12}\text{C}/^{13}\text{C}$ as a function of the luminosity in our models with observations for field low-mass metal poor stars. During the main sequence, the evolution is the

same (no modification of the surface abundances for these elements) and the lines are superimposed in the graphs. Then, the action of the rotational mixing at the base of the convective envelope during the deepening of the convective envelope on the subgiant branch and lower RGB leads to a deeper DUP. As a result, larger variations of C, N and $^{12}\text{C}/^{13}\text{C}$ are obtained at the completion of the 1st DUP in models **B** and **C** compared to model **A**, even though the difference between models **A** and **B** is hardly noticeable on the figure. Beyond this point, no other surface abundance variation is observed neither for model **B** nor for model **C**, which is in contradiction with the observational data. Indeed, although the shear mixing connects the convective envelope to the outer HBS, the total diffusion coefficient remains too small ($D_{\text{tot}} \simeq 10^8 \text{ cm}^2\text{s}^{-1}$ below the convective envelope and $5.10^4 \text{ cm}^2\text{s}^{-1}$ near the HBS in model **C**) to allow noticeable modifications to the surface abundance patterns at the bump.

4 Conclusions and Perspectives

The very first models of rotating low-mass stars including a self-consistent treatment of the transport of angular momentum and chemicals due to meridional circulation and shear turbulence, indicate that moderate diffusion of the chemicals dominated by the shear instability exists in the radiative interior at all times, and lowers the mean molecular weight barrier built at the end of the 1st DUP. These computations also show that differential rotation in the convective envelope favours an efficient turbulence and a strong mixing in the underlying radiative region. However, shear mixing alone does not allow to reproduce the observed abundance patterns in low-mass RGB stars, contrary to the claim of Denissenkov & Tout (2000).

These results raise the questions of the nature of the rotation regime of extended cool convective envelopes, the possibility for other hydrodynamical instabilities to develop inside RGB stars, and the efficiency of other physical processes (internal gravity waves, magnetic field) to transport angular momentum and chemicals in low-mass RGB stars.

References

- Charbonnel, C., 1995, ApJL, 453, L41
- Denissenkov, P.A. and Tout, C.A., 2000, MNRAS, 316, 395
- Gratton, R.G., Sneden, C., Carretta, E., Bragaglia, A., 2000, A&A, 354, 169
- Maeder A. and Zahn, J.-P. 1998, A&A, 334, 1000
- Mathis, S., Palacios, A., Zahn, J.-P. 2004, A&A, 425, 243
- Palacios, A., Charbonnel, C., Talon, S. Siess, L., 2005, A&A, submitted
- Sills, A. and Pinsonneault, M. 2000, ApJ, 540, 489
- Sweigart, A.V. and Mengel, J.G. 1979, ApJ, 229, 624.
- Talon, S. and Zahn, J.-P. 1997, A&A, 317, 749
- Zahn, J.-P., 1992, A&A, 265, 115